Elucidating the potassium-binding site and ion-coupled transport mechanism of the serotonin transporter

Jiaxin Tan[1,2,*], Yuan Xiao[1,2], Fang Kong[1,2], Tianwei Zhao[1], Yafei Yuan[1,*] and Chuangye Yan[1,*]

[1] Beijing Frontier Research Center for Biological Structure, Beijing Advanced Innovation Center for Structural Biology, State Key Laboratory of Membrane Biology, Tsinghua-Peking Joint Center for Life Sciences, School of Life Sciences, Tsinghua University, Beijing 100084, China

[2] These authors contributed equally to this work.

[*]Corresponding author. Email: tjx@mail.tsinghua.edu.cn (J. T.), yuanyf@mail.tsinghua.edu.cn (Y. Y.), yancy2019@tsinghua.edu.cn **(C.Y.)**

Abstract

The serotonin transporter (SERT) is responsible for the reuptake of the neurotransmitter serotonin (5-HT), utilizing the Na^+ gradient across the cell membrane to drive substrate transport. It is proposed that 5-HT is cotransported with one Na^+ and one Cl^-, while a potassium ion (K^+) is transported in the opposite direction. Despite recent structural advances in SERT, the precise intracellular K^+ binding site still requires experimental structural confirmation. In this study, we capture two previously unreported states of SERT: an inward-open conformation bound with one K^+ ion and one Cl^- ion, and an outward-open conformation free of any ions. These findings provide comprehensive insights into the ion-coupled transport cycle of SERT.

Introduction

Monoamine neurotransmitters, including serotonin (5-HT), dopamine (DA), and norepinephrine (NE)[1], play essential roles in regulating mood, emotion, and cognition[2]. The clearance of monoamine neurotransmitters from the synaptic cleft following neuronal signaling is mediated by the serotonin transporter (SERT), dopamine transporter (DAT), and norepinephrine transporter (NET)[2]. All monoamine transporters (MATs) belong to the Neurotransmitter: Sodium Symporter (NSS) family，whose members share two conserved sodium ion (Na^+) binding sites (Na1 and Na2) and one conserved chloride ion (Cl^-) binding site, utilizing the Na^+ gradient across the cell membrane to drive substrate transport[3].

The substrate: ion stoichiometry and energy coupling model of SERT were first established in 1978, proposing that 5-HT is cotransported with one Na^+ and one Cl^-, while a potassium ion (K^+) is transported in the opposite direction[4]. The currently accepted mechanism is as follows: Na^+ binding stabilizes the outward-open conformation of SERT[5,6]; subsequent binding of extracellular Cl^- together with 5-HT^+ triggers the transition to the inward-open state[7,8]; on the intracellular side, 5-HT^+ and Na^+ dissociate, completing their coupled transmembrane transport[9]. To reset SERT to the outward-open conformation, intracellular K^+ must bind, displace Na^+, and drive the return to the initial state[4,10,11].

Although Na^+/5-HT cotransport is well established, the precise roles of K^+ and Cl^- have long been debated. Later studies showed that K^+ efflux is coupled to SERT activity:

intracellular K^+ accelerates the inward-to-outward conformational reset and thus promotes turnover, whereas extracellular K^+ may inhibit transport by competing with Na^+ at binding sites[10,12,13]. Because reset is considered the rate-limiting step of the cycle, K^+ antiport is a key determinant of SERT efficiency. Strong evidence comes from experiments demonstrating that an outward K^+ gradient alone can drive 5-HT accumulation, directly supporting a mechanistic role for K^+[12]. Moreover, other monoamine transporters (MATs) and the bacterial leucine transporter LeuT have been shown to bind intracellular K^+[14-17]; however, within the NSS family, SERT remains the only member experimentally proven to couple intracellular K^+ to transport. With respect to Cl^-, its requirement for substrate transport by SERT and other NSS members is well established. Early studies suggested that SERT might symport Cl^- with 5-HT^+, with the Cl^- gradient neutralizing the positive charge of co-transported Na^+ to maintain electroneutrality and facilitate transport[18-20]; Cl^- binding has also been proposed to induce necessary conformational changes[21]. More recent data indicate that intracellular Cl^- does not affect the transmembrane current associated with 5-HT^+ transport; SERT does not co-transport Cl^- as a coupled substrate but nonetheless requires extracellular Cl^- binding for normal function[12,22].

Despite substantial insight into SERT's ion-coupling mechanism, key structural questions remain. First, the precise K^+ binding site has not been directly visualized in existing structures. Functional and computational studies suggest that K^+ may occupy the core second sodium site (Na2) after substrate and Na^+ release to drive the inward-to-outward reset, but direct structural evidence is still lacking[11]. Second, the fate of Cl^-

during the transport cycle remains disputed: some studies propose that Cl^- stays bound to SERT throughout the cycle [12], yet this hypothesis—and the specific role of Cl^- in conformational transitions and energy coupling—requires further experimental validation[13].

In our previous study on the structure of NET in the presence of the antidepressant desipramine, we identified additional density at the Na1 site corresponding to K^+. This finding marked the first visualization of K^+ ions within the NSS family[15]. Furthermore, we observed the absence of Cl^- density in the inward-open conformation of NET in the presence of NE, supporting the hypothesis that Cl^- release is a critical step in the transport cycle. However, questions remain regarding the binding site of K^+ ions and the potential release of Cl^- in SERT. To address these uncertainties and to validate whether our conclusions of NET are generalizable within the MAT family, we performed structural determination of SERT using purification steps similar to those employed for NET.

Here, we identified two previously unreported states of SERT: an inward-open conformation bound with one K^+ ion and one Cl^- ion, and an outward-open conformation devoid of any ions. Additionally, we achieved higher resolution structures of the outward-open conformation of SERT bound with Na^+ and Cl^- ions. These findings provide valuable insights into the ion-coupled transport cycle of SERT.

Results

Structure determination of SERT

The human SERT construct, fused with an N-terminal FLAG tag, was transiently expressed in HEK293F cells. After purification using anti-FLAG affinity resin, the SERT protein underwent size-exclusion chromatography (SEC) on a Superose 6 column in the presence of 0.02% (w/v) n-dodecyl-β-d-maltoside (DDM) (Supplementary Fig. S1). We successfully determined three structures of SERT in DDM detergent under both NaCl and KCl conditions at resolution of 2.9 to 3.2 Å (Fig. 1a-c, Supplementary Fig. S2-4). The high-quality electron microscopy map enabled the assignment of approximately 540 side chains of SERT along with its corresponding substrate (Supplementary Fig. S5). Detailed information regarding sample preparation and data processing can be found in the Methods section.

Consistent with previous studies in NaCl condition[23], we solved an outward-open structure of SERT bound to Na^+ and Cl^- ions and two substrate 5-HT molecules (referred to as SERT-NaCl-OO) (Fig. 1a, Supplementary Fig. S2). In this structure, the density of Na^+ in the Na2 site was much stronger than at the Na1 site (Fig. 1d). Interestingly, in KCl conditions, we capture two previously unreported states of SERT: an inward-open conformation with one K^+ ion and one Cl^- ion (referred to as SERT-KCl-IO), and an outward-open conformation free of any ions (referred to as SERT-KCl-OO) (Fig. 1b-c, e-f, Supplementary Fig. S3). A comparison of these two structures in KCl conditions clearly revealed the absence of Na^+, K^+, and Cl^- densities in the

outward-open conformation, suggesting that substrate binding may occur before ion binding in the outward-open state (Fig. 1c, f). This is also the first time the ion-free state of SERT has been captured. In contrast, additional density corresponding to K^+ at the Na1 site was observed in the inward-open conformation, marking the first visualization of a K^+ ion within the SERT (Fig. 1b, e).

The Na^+, K^+ and Cl^- binding sites

With comparable resolutions of the three structures, we performed a detailed analysis of the Na^+ and Cl^- binding sites. Comparing SERT-KCl-OO with SERT-NaCl-OO revealed slight structural changes in chelating residues upon Na^+ and Cl^- binding (Fig. 2a). Specifically, in the Na1 site, the side chains of Asn101 and Ser336 shift and flip for chelating a Na^+ ion. In the Na2 site, the side chain of Asp437 undergoes a flip to chelate another Na^+ ion. Regarding the Cl^- binding site, the hydroxyl group of Ser336 flips to coordinates Cl^- ion.

In contrast, comparing SERT-NaCl-OO with SERT-KCl-IO revealed structural changes in chelating residues upon ion release (Fig. 2b). In the Na1 site, key residues such as Ala96 rotate and move outward by 4.4 Å, disrupting Na^+ coordination and creating space for K^+ ion binding. The newly formed chelating bonds have an average length of 2.8 Å, ideal for K^+ ions compared to 2.3 Å for Na^+ ions. In the Na2 site, Asp437 flips away from chelating Na^+ ion, leading to its release. In Cl^- binding site, the coordination of Cl^- remains largely unchanged.

Comparison of the K^+ ion binding site of NET and SERT

To further explore the K^+ binding of Na1 site, we compared the structures of SERT-KCl-IO, the occluded NET in NaCl (NET-NaCl-OC) (PDB codes: 8WGR), and the inward-open NET in KCl (NET-KCl-IO) (PDB code: 8ZPB). During the transition from the occluded to the inward-facing state, Na^+-chelating residues such as Ala96 in the Na1 site undergo similar structural adjustments as observed between SERT-NaCl-OO and SERT-KCl-IO. These rearrangements in the Na1 site facilitate the accommodation of K^+ instead of Na^+ (Fig. 3a). In both inward-open states of SERT and NET in KCl, the organization of Na1 is similar, highlighting strong structural consistency of the conserved K^+-binding site across the NSS family (Fig.3b).

Proposed ion-coupled transport cycle of SERT

The ion-free outward-open structure of SERT-KCl-OO provides compelling evidence that substrate binding can occur before ion binding in this conformation. This observation, along with the absence of Cl^- density in the inward-open structure of NET in the present of NE in NaCl[15], further strengthens the notion that Cl^- release is a key step in the transport cycle. Additionally, the inward-open structures of SERT and NET in KCl suggest that K^+ plays a crucial role in facilitating the transition from the inward-open to the outward-open state. Building on these findings and previous models of SERT transport[24], we propose a more refined and comprehensive model for the ion-coupled transport cycle of SERT (Fig. 4).

The transport cycle initiates with SERT in an outward-open conformation where substrate binding may precede ion binding; in addition to the central pocket, the

allosteric site is also occupied by a second 5-HT molecule during the transport. After substrate binding, Na^+ and Cl^- ions bind to their respective sites, triggering the transition to the occluded state. The transporter then undergoes a conformational change to the inward-facing state, opening transmembrane helix 1a (TM1a), which facilitates the release of Na^+ ions into the cytosol. Subsequently, K^+ binds to the Na1 site, further facilitating the transition. During this phase, both the central substrate and Cl^- ion are released. Following substrate release, the transporter transitions back to the outward-facing state via another occluded intermediate. In the outward-facing state, K^+ ion is released, and the central site is primed to rebind 5-HT, either from the extracellular space or, more efficiently, from the allosteric 5-HT site, preparing SERT for the next round of transport.

Discussion

Our structural study provides new insights into the long-standing debate surrounding the roles of K^+ and Cl^- in the serotonin transporter (SERT) transport cycle. We captured two novel conformations of SERT: one in which K^+ (at the Na1 site) and Cl^- are bound in an inward-open conformation, and another that is devoid of ions, representing the outward-open state. Additionally, we observed the classic outward-open state with Na^+/Cl^- binding. These structures reveal critical steps in the SERT ion-coupling mechanism, allowing us to propose a more refined transport cycle model that addresses two unresolved issues since the 1970s.

Functional studies have long demonstrated the essential role of intracellular K^+ in SERT resetting, but the precise binding site has remained unclear. Previous computational and mutation studies have localized the K^+ binding site to Na2, with mutations at this site eliminating K^+ (or H^+) driven uptake[11]. However, for the first time, we directly observed K^+ stably bound at the Na1 site in the inward-open SERT-KCl-IO cryo-EM structure, while the Na2 site was vacant. In this conformation, the Na1 site is expanded by approximately 4.4 Å due to the movement of Ala96, making it more suitable for coordinating the larger K^+ ion. This finding contrasts with earlier studies, likely due to differences in the captured transporter conformations. Our cryo-EM directly captured the inward-open state, where the key residue at Na2 (Asp437) is flipped away, preventing it from coordinating K^+. In contrast, previous simulations and functional studies primarily focused on the dynamic process of transition from the outward-closed to inward-facing state, where the Na2 residue might temporarily coordinate K^+. This conformation dependence suggests that K^+ binding is a dynamic process, potentially favoring different binding sites during different stages of the transport cycle, ultimately stabilizing at Na1 to drive transporter resetting. Future studies combining more dynamic analyses and multi-state structural captures will provide a more comprehensive understanding of K^+'s role in the SERT cycle. Both SERT and NET[15] show K^+ binding at Na1, and studies on the homologous NSS family bacterial protein LeuT also report that K^+ affinity is sensitive to mutations at the Na1

site[17]. Together, these results support Na1 as the conserved K^+ binding site within the NSS family.

The dependency of SERT on chloride ions (Cl^-) has been a focal point in monoamine transporter research. Although early stoichiometric models proposed Cl^- as a co-transported ion with the substrate[22], subsequent functional studies have shown that, while Cl^- is essential for transport activity, it does not co-transport with the substrate[12,22]. Our analysis of the ion-free outward-open conformation (SERT-KCl-OO) further supports this view, as it captures the substrate binding intermediate state in the absence of ions, indicating that 5-HT binding may precede ion binding to initiate the transport cycle. This finding challenges the conventional model that assumes strict ion binding in a specific order (Na^+ first)[25,26], and aligns with earlier biochemical studies showing that SERT and other monoamine transporters can bind substrate in the absence of Na^+ or Cl^-, though full transport cannot occur without ions[13,27]. Notably, while SERT's homologous proteins, such as LeuT, use negatively charged amino acids to replace Cl^-[19,28,29], SERT and other monoamine transporters have evolved a dependence on exogenous Cl^-. This suggests that Cl^- plays a unique structural cofactor role in these transporters. We propose that Cl^- binds externally at the beginning of each transport cycle to stabilize the transporter's conformation, thereby facilitating efficient substrate uptake. Cl^- is then released from the internal side at the end of the cycle, driven by conformational rearrangements, preparing the transporter for the next round of transport.

In summary, the high-resolution structures of human SERT analyzed under NaCl and KCl conditions, particularly the two distinct states observed under KCl conditions, provide the first structural evidence of K^+ binding and Cl^- release during the SERT transport cycle. The identification of the K^+ binding site and the observation of Cl^- release complement previous findings of K^+ binding in NET[15], filling a crucial gap in our understanding of SERT ion-coupling mechanisms. Our structures reveal a potentially conserved ion-coupling mechanism within the monoamine transporter (MAT) family, offering a more complete picture of how ion gradients drive neurotransmitter uptake. These findings provide a critical foundation for future research and may inform the design of drugs targeting these essential proteins in neuropsychiatric conditions.

Acknowledgements

We thank the Tsinghua University Branch of China National Center for Protein Sciences (Beijing) for providing the cryo-EM facility support and the computational facility support. This work was funded by the National Natural Science Foundation of China (32171204, C.Y), the National Key R&D Program of China (2020YFA0509301, C.Y.), and the Tsinghua University Initiative Scientific Research Program (20221080032, 20231080037, C.Y), Beijing Frontier Research Center for Biological Structure, and Start-up funds from Tsinghua-Peking Center for Life Sciences and Tsinghua University.

Author Contributions: C.Y, J.T. and Y.Y. conceived the project. J.T. and C.Y. designed all experiments. J.T., Y.X. and T.Z. performed the experiments. F.K. and C.Y. contributed to the data processing and structure determination. All authors contributed to manuscript preparation. J.T. and C.Y. wrote the manuscript.

Conflict of Interest Statement: The authors declare no competing interests.

Figures and legends

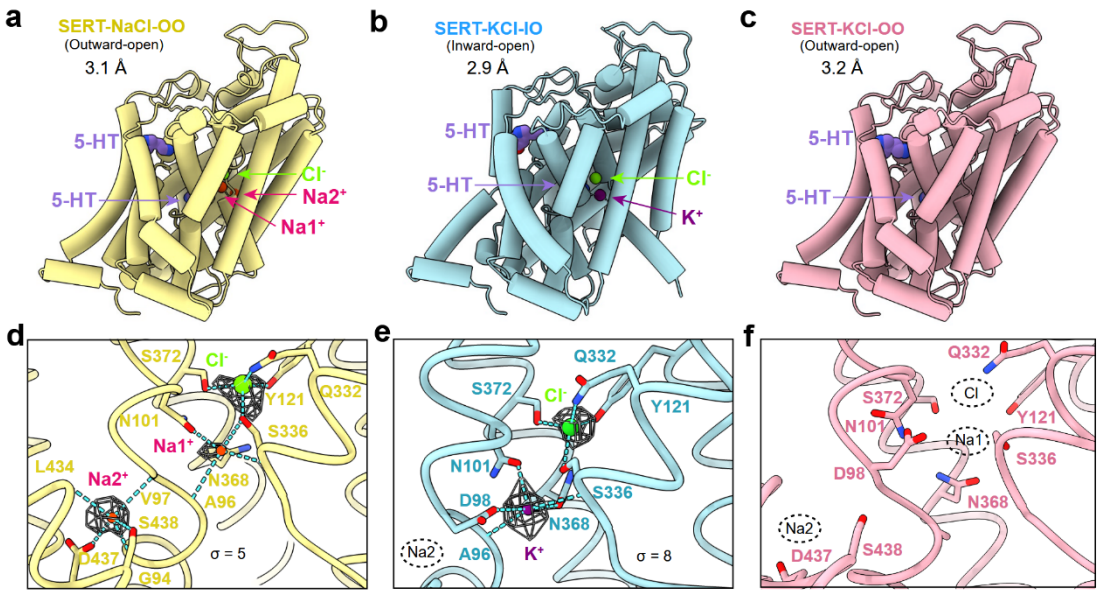

Fig. 1| The SERT structures in different states. a-c, The SERT structures in different states. *Panel a*: SERT-NaCl-OO (yellow color), the outward-open structure of SERT bound to 5-HT in a NaCl solution. *Panel b* SERT-KCl-IO (cyan color), the inward-open structure of SERT bound to 5-HT in a KCl solution. *Panel c*: SERT-KCl-OO (pink color), the outward-open structure of SERT bound to 5-HT in a KCl solution. The Na^+, K^+, Cl^-, and 5-HT are represented as red, purple, green, and slate blue spheres, respectively. **d-f**, The ion binding site and cryo-EM densities of SERT. The cryo-EM densities and coordination of Na1, Na2, and Cl^- binding sites are shown for the structures of SERT-NaCl-OO (*panel d*), SERT-KCl-IO (*panel e*), and SERT-KCl-OO (*panel f*). In the SERT-KCl-IO structure, K^+ density is observed at the Na1 site. In the SERT-KCl-OO structure, there are no densities for Na^+, K^+, and Cl^-.

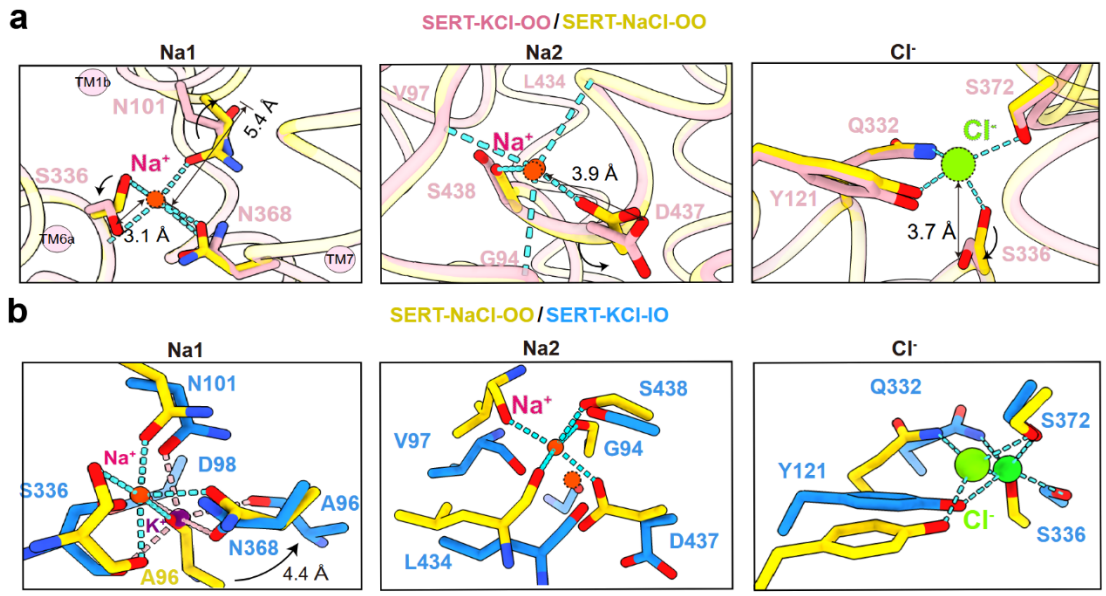

Fig. 2| Comparison of the ion binding sites. **a**, Comparison of the ion binding sites between SERT-KCl-OO and SERT-NaCl-OO. SERT-KCl-OO and SERT-NaCl-OO are colored pink and yellow, respectively. *Left panel*: in the Na1 site, the side chains of Asn101 and Ser336 flips upon Na^+ binding. *Middle panel*: in the Na2 site, the carboxyl group of Asp437 swings back upon Na^+ binding. *Right panel*: in the Cl^- binding site, the hydroxyl group of Ser336 flips for coordination of Cl^- ion. **b**, Comparison of the ion binding sites between SERT-NaCl-OO and SERT-KCl-IO. SERT-NaCl-OO and SERT-KCl-IO are colored yellow and marine, respectively. *Left panel*: in the Na1 site, Ala96 rotates and shifts outward by 4.4 Å, creating space for K^+ accommodation. The hydroxyl group of Ser336 no longer coordinates with K^+. *Middle panel*: in the Na2 site, the carboxyl group of Asp437 swings away to release Na^+. *Right panel*: in the Cl^- binding site, the coordination of Cl^- ion is generally the same.

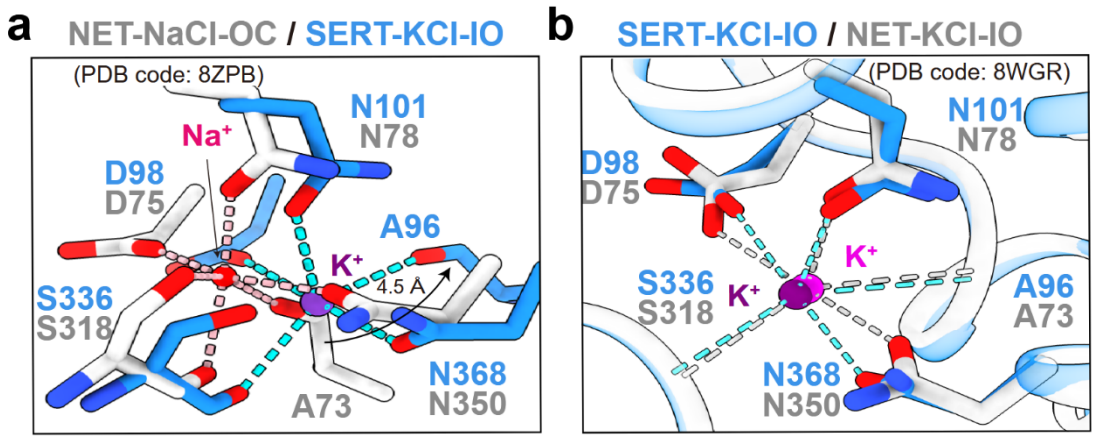

Fig. 3| Comparison the Na1 site between SERT and NET. **a**, Comparison of the Na1 site between the occluded conformation of NET in NaCl (PDB code: 8ZP8) and SERT-KCl-IO. SERT and NET are colored marine and light gray, respectively. During the transition from occluded to inward-facing, Ala96 rotates and shifts outward by 4.5 Å, creating space for K^+ accommodation. **b**, Comparison of the Na1 site between the inward-open conformation of NET in KCl (PDB code: 8WGR) and SERT-KCl-IO. The coordination of K^+ is similar between SERT and NET.

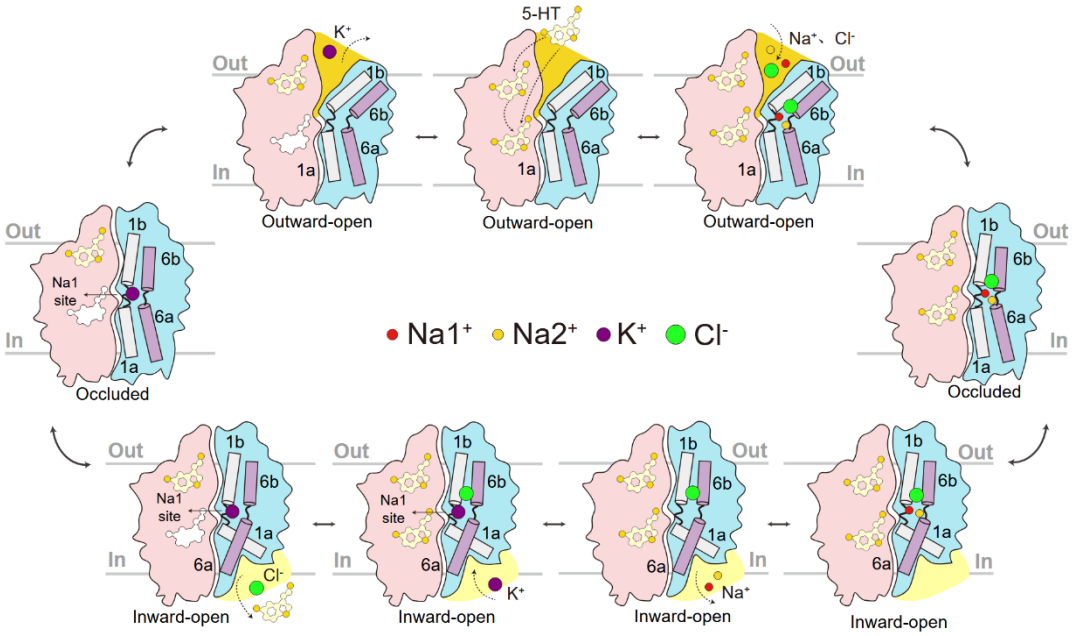

Fig. 4| Proposed ion-coupled transport cycle of SERT. Cartoon representation of the ion-coupled transport cycle of SERT. The scaffold domain is shown in pink and the core domain in blue. TM1 and TM6 are highlighted in light gray and purple, respectively. Na^+, $Na2^+$, Cl^-, and K^+ are depicted as red, light yellow, purple, and green spheres, respectively.

Methods

Cell Culture

The *Escherichia coli* strain DH5α was cultured in LB medium (Sigma) at 37 ℃ at 37 °C for the generation and amplification of plasmids for SERT and its mutant. Mammalian HEK293F cells were maintained in SMM 293-TII medium (Sino Biological) at 37 °C with 5% CO_2 to facilitate protein expression.

Protein expression and purification

The full-length, wild-type human SERT cDNA (UniProt ID: P31645) was inserted into a pCAG vector at the KpnI and XhoI sites with an N-terminal FLAG tag. SERT F311A mutant was generated using a standard PCR-based approach. SERT overexpression was performed in HEK293F cells, with 2 mg of plasmid and 4 mg of polyethylenimine (Polysciences) pre-incubated in 50 ml of fresh SMM 293-TII medium for 15 minutes before adding to one liter of HEK293F cells at a density of 2.0×10^6 cells/ml. The cells were cultured for 48 hours at 37 °C, 5% CO_2, shaking at 220 rpm. Cells were harvested by centrifugation, resuspended in lysis buffer (20 mM Tris-HCl pH 8.0, 150 mM NaCl). The SERT mutant F311A were resuspended in 20 mM Tris-HCl pH 8.0, 150 mM KCl, then frozen in liquid nitrogen and stored at -80 °C for later use.

For protein purification, cell pellet was thawed on ice, and cell membrane was solubilized in lysis buffer containing protease inhibitors (5 μg/ml aprotinin, 1 μg/ml pepstatin, and 5 μg/ml leupeptin; Amresco) and 2% (w/v) DDM (Anatrace) at 4 °C for

2 h, followed by centrifugation at 20,000 g at 4 °C for 1 h. The supernatant was loaded on anti-FLAG M2 resin (Sigma). The resin was then washed with 15 column volumes (CV) of wash buffer containing 20 mM Tris-HCl pH 8.0, 150 mM NaCl, and 0.02% (w/v) DDM. The protein was eluted with 6 CV of wash buffer plus 0.4 mg/ml FLAG peptide at 4 °C. The elution was concentrated before further purification by size-exclusion chromatography (Superose 6 Increase 10/300 GL column; GE Healthcare) in the buffer containing 20 mM Tris-HCl pH 8.0, 150 mM NaCl, and 0.02% (w/v) DDM. The peak fractions were collected and concentrated for subsequent experiments. The SERT-KCl proteins (F311A) were prepared in buffers containing 20 mM Tris-HCl pH 8.0, 150 mM KCl, and 0.02% (w/v) DDM in the whole process.

Cryo-EM sample preparation and data acquisition

For cryo-EM sample preparation, 4 μl of purified SERT protein, concentrated to ~10 mg/ml, was applied to glow-discharged Quantifoil holey carbon grids (Quantifoil Au R1.2/1.3, 300 mesh). Proteins (SERT-NaCl and SERT-KCl) were incubated with 15 mM serotonin for 30min before freezing. Grids were blotted for 3.5 s at 4 °C with 100% humidity and plunge-frozen in liquid ethane using a Vitrobot (Mark IV, Thermo Fisher Scientific).

Cryo-EM data were acquired on a 300 kV Titan Krios G3i with a Gatan K3 detector and a GIF Quantum energy filter (20 eV slit width). Defocus ranged from -1.4 to -1.8 μm. Each 32-frame stack was exposed for 2.56 s, with each frame exposed for 0.08 s. Micrographs were collected using the AutoEMation program[30] in super-

resolution counting mode, with a binned pixel size of 1.083 Å, and a total dose of ~50 e-/Å^2. The frames in each stack were aligned and summed using MotionCor2[31].

Data processing

All dose-weighted micrographs underwent manual inspection, with low-quality ones excluded before import into cryoSPARC[32]. The Contrast Transfer Function (CTF) parameters were estimated using Patch-CTF. Initial 2D templates were generated using particles picked by Blob Picker, followed by Template Picker for subsequent all particle picking tasks. Particles were initially extracted with a box size of 192 pixels and subsequently cropped to 96 pixels to accelerate computation.

For the SERT-NaCl and SERT-KCl datasets, 4,702,874 and 4,796,961 particles were extracted from 3,142 and 1,817 micrographs, respectively. Initial references were generated using good particles selected after 2D classification. The major conformation in SERT-NaCl dataset is outward-open, while in SERT-KCl dataset it is inward-open. Using skip-alignment 3D classification, a minor outward-open conformation was identified in the SERT-KCl dataset. After several rounds of 3D classification, 251,580 (SERT-NaCl-OO), 671,549 (SERT-KCl-IO) and 163,535 (SERT-KCl-OO) particles were retained for Non-Uniform refinement and local refinement, achieving resolutions of 3.10, 2.88 and 3.22 Å, respectively.

Model building and refinement

Both the outward-open (PDB code: 7LIA) and inward-open (PDB code: 7LI9)

structures of SERT were used as initial models, which were fitted into the corresponding cryo-EM maps using ChimeraX[33]. Manual adjustments and rebuilding were performed using COOT[34]. The final models of all datasets were refined against the corresponding maps using PHENIX in real space with secondary structure and geometry restraints[35]. Overfitting of the model was monitored by refining the model in one of the two independent half maps from the gold-standard refinement approach, and testing the refined model against the other half map[36]. The structures were validated through examination of the Clash scores, Molprobity scores, and statistics of the Ramachandran plots by PHENIX[37].

Data Availability

Atomic coordinates of SERT-NaCl-OO, SERT-KCl-OO and SERT-KCl-IO have been deposited in the Protein Data Bank under the accession codes 8WHF, 8WHD and 8WHE, respectively. The corresponding electron microscopy maps have been deposited in the Electron Microscopy Data Bank under the accession codes EMD-37542, EMD-37540, and EMD-37541, respectively.

References

1. Roth, K.A., Mefford, I.M. & Barchas, J.D. Epinephrine, norepinephrine, dopamine and serotonin: differential effects of acute and chronic stress on regional brain amines. *Brain Res* **239**, 417-24 (1982).

2. Torres, G.E., Gainetdinov, R.R. & Caron, M.G. Plasma membrane monoamine transporters: structure, regulation and function. *Nat Rev Neurosci* **4**, 13-25 (2003).

3. Cheng, M.H. & Bahar, I. Monoamine transporters: structure, intrinsic dynamics and allosteric regulation. *Nat Struct Mol Biol* **26**, 545-556 (2019).

4. Rudnick, G. & Nelson, P.J. Platelet 5-hydroxytryptamine transport, an electroneutral mechanism coupled to potassium. *Biochemistry* **17**, 4739-42 (1978).

5. Fenollar-Ferrer, C. et al. Structure and regulatory interactions of the cytoplasmic terminal domains of serotonin transporter. *Biochemistry* **53**, 5444-60 (2014).

6. Tavoulari, S. et al. Two Na+ Sites Control Conformational Change in a Neurotransmitter Transporter Homolog. *J Biol Chem* **291**, 1456-71 (2016).

7. Zhang, Y.W. & Rudnick, G. The cytoplasmic substrate permeation pathway of serotonin transporter. *J Biol Chem* **281**, 36213-20 (2006).

8. Schicker, K. et al. Unifying concept of serotonin transporter-associated currents. *J Biol Chem* **287**, 438-445 (2012).

9. Talvenheimo, J., Fishkes, H., Nelson, P.J. & Rudnick, G. The serotonin transporter-imipramine "receptor". *J Biol Chem* **258**, 6115-9 (1983).

10. Nelson, P.J. & Rudnick, G. Coupling between platelet 5-hydroxytryptamine and potassium transport. *J Biol Chem* **254**, 10084-9 (1979).

11. Hellsberg, E. et al. Identification of the potassium-binding site in serotonin transporter. *Proc Natl Acad Sci U S A* **121**, e2319384121 (2024).

12. Hasenhuetl, P.S., Freissmuth, M. & Sandtner, W. Electrogenic Binding of Intracellular Cations Defines a Kinetic Decision Point in the Transport Cycle of the Human Serotonin Transporter. *J Biol Chem* **291**, 25864-25876 (2016).

13. Rudnick, G. & Sandtner, W. Serotonin transport in the 21st century. *J Gen Physiol* **151**, 1248-1264 (2019).

14. Schmidt, S.G. et al. The dopamine transporter antiports potassium to increase the uptake of

dopamine. *Nat Commun* **13**, 2446 (2022).

15. Tan, J. et al. Molecular basis of human noradrenaline transporter reuptake and inhibition. *Nature* **632**, 921-929 (2024).

16. Billesbølle, C.B. et al. Transition metal ion FRET uncovers K(+) regulation of a neurotransmitter/sodium symporter. *Nat Commun* **7**, 12755 (2016).

17. Schmidt, S.G., Nygaard, A., Mindell, J.A. & Loland, C.J. Exploring the K(+) binding site and its coupling to transport in the neurotransmitter:sodium symporter LeuT. *Elife* **12**(2024).

18. Marazziti, D. et al. The role of platelet/lymphocyte serotonin transporter in depression and beyond. *Curr Drug Targets* **14**, 522-30 (2013).

19. Zomot, E. et al. Mechanism of chloride interaction with neurotransmitter:sodium symporters. *Nature* **449**, 726-30 (2007).

20. Nelson, P.J. & Rudnick, G. The role of chloride ion in platelet serotonin transport. *J Biol Chem* **257**, 6151-5 (1982).

21. Zhang, Y.W. et al. Chloride-dependent conformational changes in the GlyT1 glycine transporter. *Proc Natl Acad Sci U S A* **118**(2021).

22. Huang, J. et al. The Role of Chloride Ions in Serotonin Transport. *bioRxiv* (2025).

23. Coleman, J.A., Green, E.M. & Gouaux, E. X-ray structures and mechanism of the human serotonin transporter. *Nature* **532**, 334-9 (2016).

24. Yang, D. & Gouaux, E. Illumination of serotonin transporter mechanism and role of the allosteric site. *Sci Adv* **7**, eabl3857 (2021).

25. Szöllősi, D. & Stockner, T. Sodium Binding Stabilizes the Outward-Open State of SERT by Limiting Bundle Domain Motions. *Cells* **11**(2022).

26. Zhang, Y.W. et al. Structural elements required for coupling ion and substrate transport in the neurotransmitter transporter homolog LeuT. *Proc Natl Acad Sci U S A* **115**, E8854-e8862 (2018).

27. Humphreys, C.J., Wall, S.C. & Rudnick, G. Ligand binding to the serotonin transporter: equilibria, kinetics, and ion dependence. *Biochemistry* **33**, 9118-25 (1994).

28. Forrest, L.R., Tavoulari, S., Zhang, Y.W., Rudnick, G. & Honig, B. Identification of a chloride ion binding site in Na+/Cl -dependent transporters. *Proc Natl Acad Sci U S A* **104**, 12761-6 (2007).

29. Tavoulari, S., Rizwan, A.N., Forrest, L.R. & Rudnick, G. Reconstructing a chloride-binding site in a bacterial neurotransmitter transporter homologue. *J Biol Chem* **286**, 2834-42 (2011).

30. Lei, J. & Frank, J. Automated acquisition of cryo-electron micrographs for single particle reconstruction on an FEI Tecnai electron microscope. *J Struct Biol* **150**, 69-80 (2005).

31. Zheng, S.Q. et al. MotionCor2: anisotropic correction of beam-induced motion for improved cryo-electron microscopy. *Nat Methods* **14**, 331-332 (2017).

32. Punjani, A., Rubinstein, J.L., Fleet, D.J. & Brubaker, M.A. cryoSPARC: algorithms for rapid unsupervised cryo-EM structure determination. *Nat Methods* **14**, 290-296 (2017).

33. Pettersen, E.F. et al. UCSF ChimeraX: Structure visualization for researchers, educators, and developers. *Protein Sci* **30**, 70-82 (2021).

34. Emsley, P. & Cowtan, K. Coot: model-building tools for molecular graphics. *Acta Crystallogr D Biol Crystallogr* **60**, 2126-32 (2004).

35. Afonine, P.V. et al. Real-space refinement in PHENIX for cryo-EM and crystallography. *Acta Crystallogr D Struct Biol* **74**, 531-544 (2018).

36. Amunts, A. et al. Structure of the yeast mitochondrial large ribosomal subunit. *Science* **343**, 1485-1489 (2014).

37. Liebschner, D. et al. Macromolecular structure determination using X-rays, neutrons and electrons: recent developments in Phenix. *Acta Crystallogr D Struct Biol* **75**, 861-877 (2019).

Supplementary Information for

Elucidating the potassium-binding site and ion-coupled transport mechanism of the serotonin transporter

Jiaxin Tan[1,2], Yuan Xiao[1,2], Fang Kong[1,2], Tianwei Zhao, Yafei Yuan[1,] and Chuangye Yan[1,*]

[1] Beijing Frontier Research Center for Biological Structure, Beijing Advanced Innovation Center for Structural Biology, State Key Laboratory of Membrane Biology, Tsinghua-Peking Joint Center for Life Sciences, School of Life Sciences, Tsinghua University, Beijing 100084, China

[2] These authors contributed equally to this work.

[*]Corresponding author. Email: tjx@mail.tsinghua.edu.cn (J. T.), yuanyf@mail.tsinghua.edu.cn (Y. Y.), yancy2019@tsinghua.edu.cn **(C.Y.)**

This PDF file includes:

Figure S1-S5

Table S1

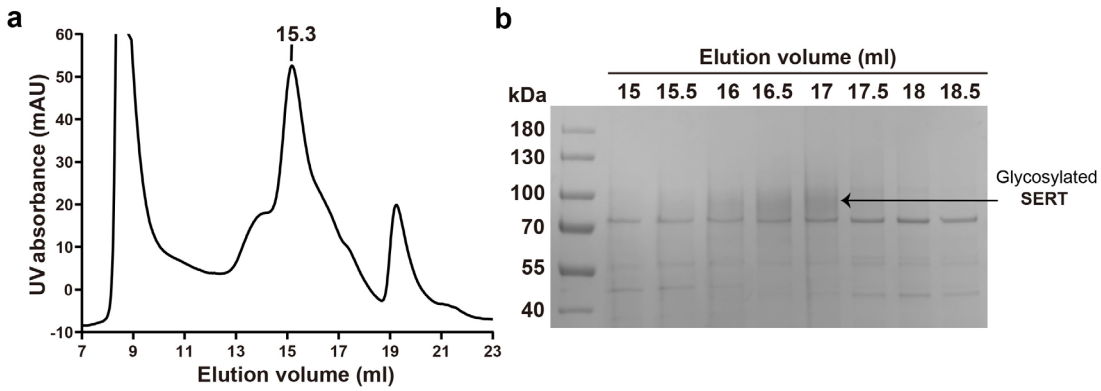

Supplementary Fig. 1 | Biochemical characterization of recombinantly expressed SERT. **a**, SEC purification of SERT in the presence of 0.02% (w/v) DDM. **b**, Peak fractions of SEC purification were further examined by Coomassie blue staining of SDS–PAGE.

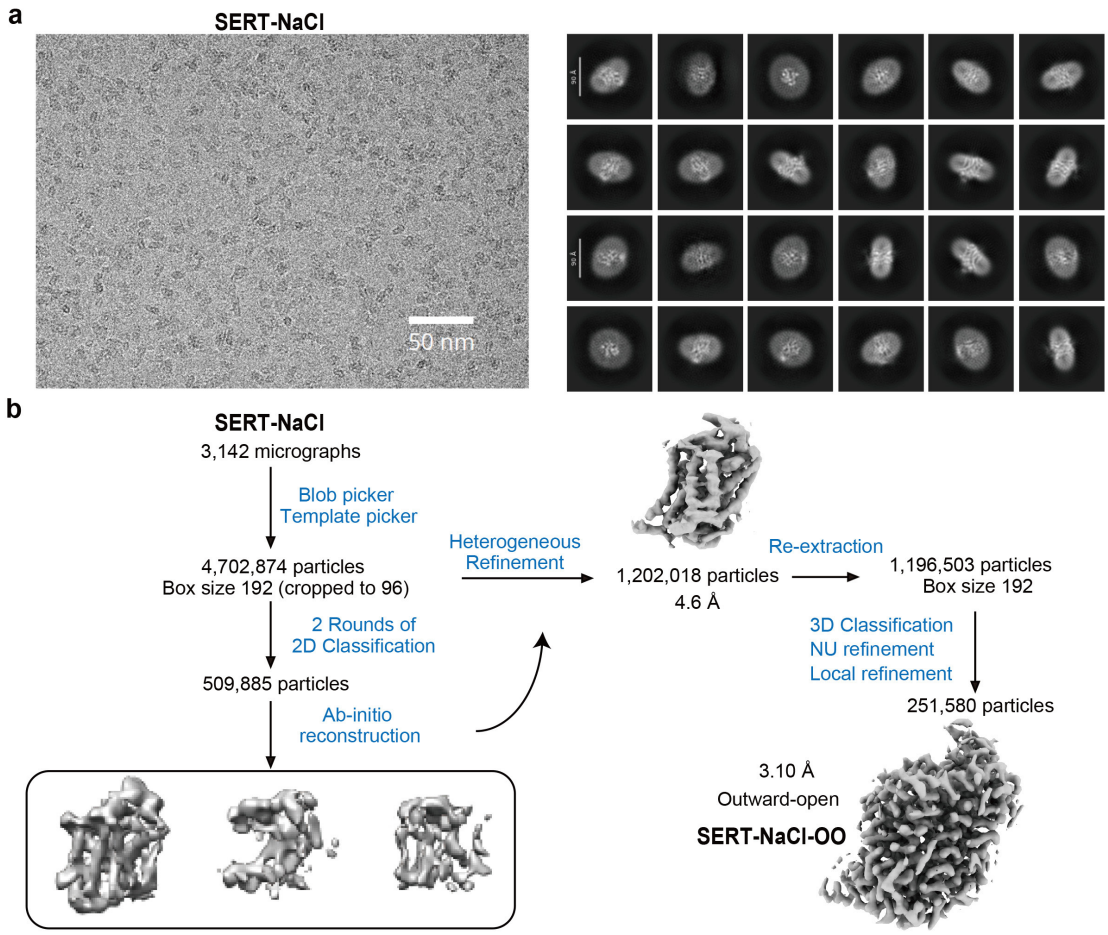

Supplementary Fig. 2 | Data processing of SERT in NaCl. **a**, Representative micrograph and 2D class averages of SERT-NaCl. **b**, The flowchart for data processing.

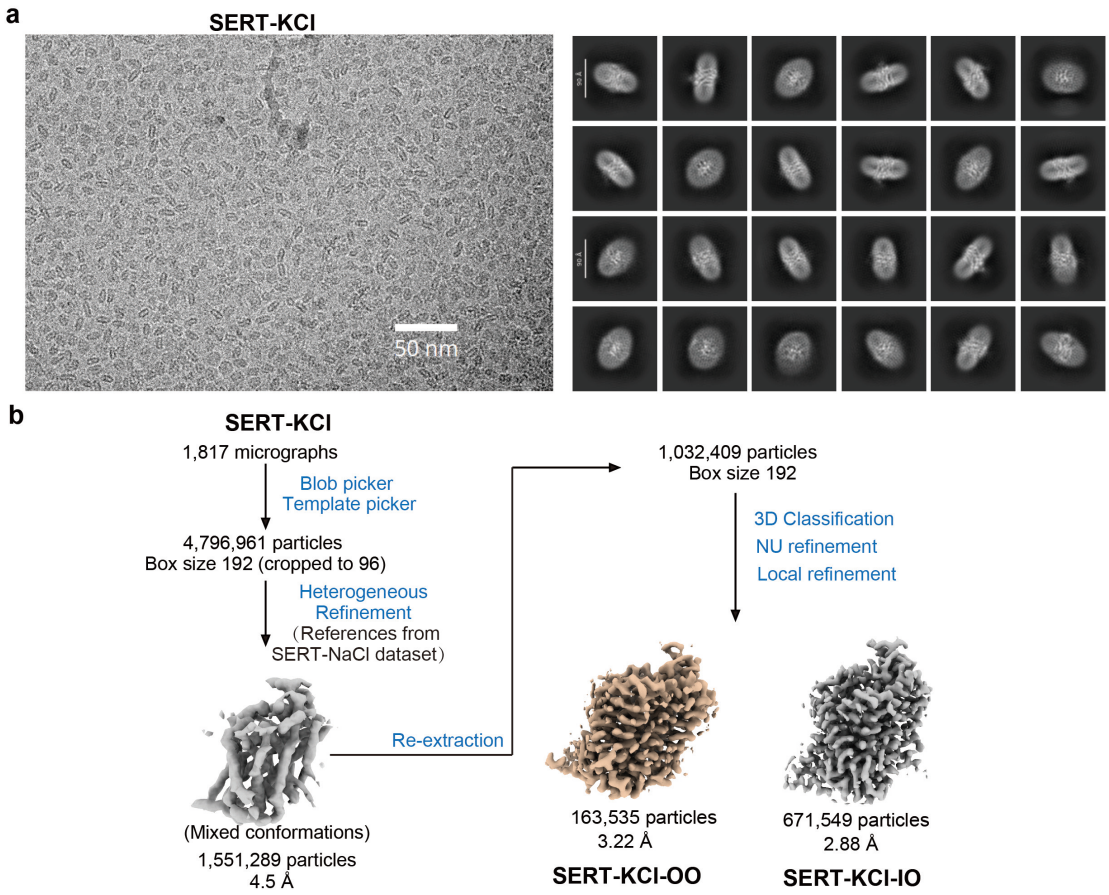

Supplementary Fig. 3 | Data processing of SERT in KCl. **a**, Representative micrograph and 2D class averages of SERT-KCl. **b**, The flowchart for data processing.

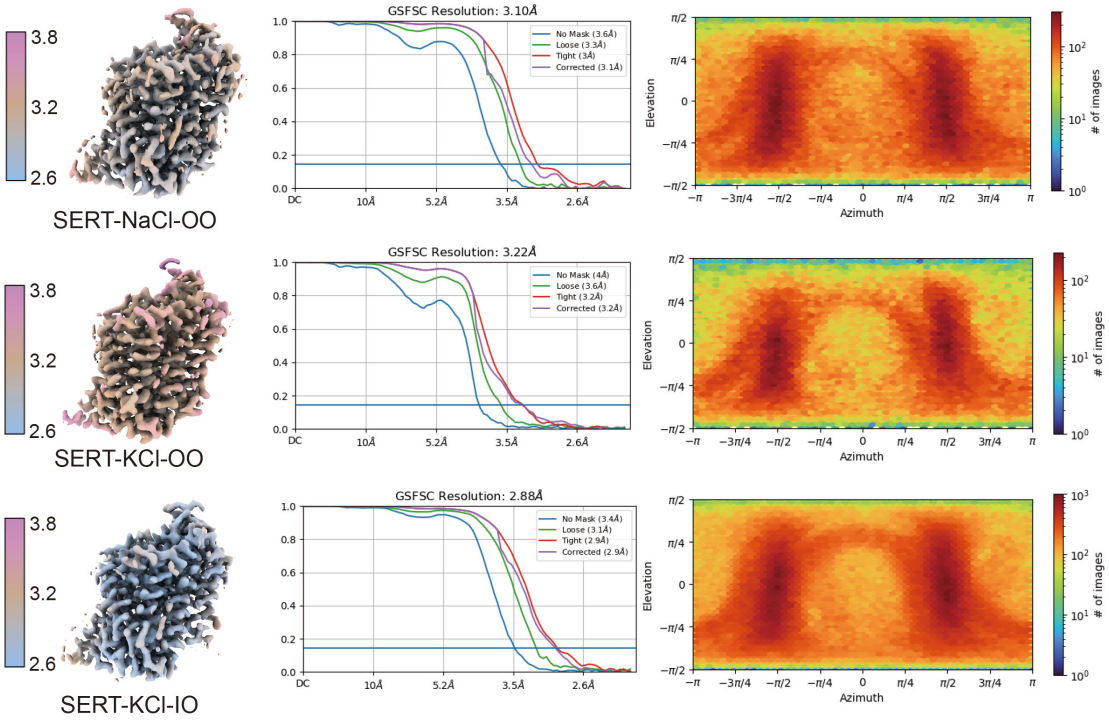

Supplementary Fig. 4 | Cryo-EM analysis of SERT. *Top panel*: SERT-NaCl-OO; *Middle panel:* SERT-KCl-OO; *Bottom panel:* SERT-KCl-IO. Various assessments of the cryo-EM reconstruction are presented, including local resolution maps, gold-standard Fourier shell correlation (FSC) curves, and angular distribution of the particles used for the final reconstruction.

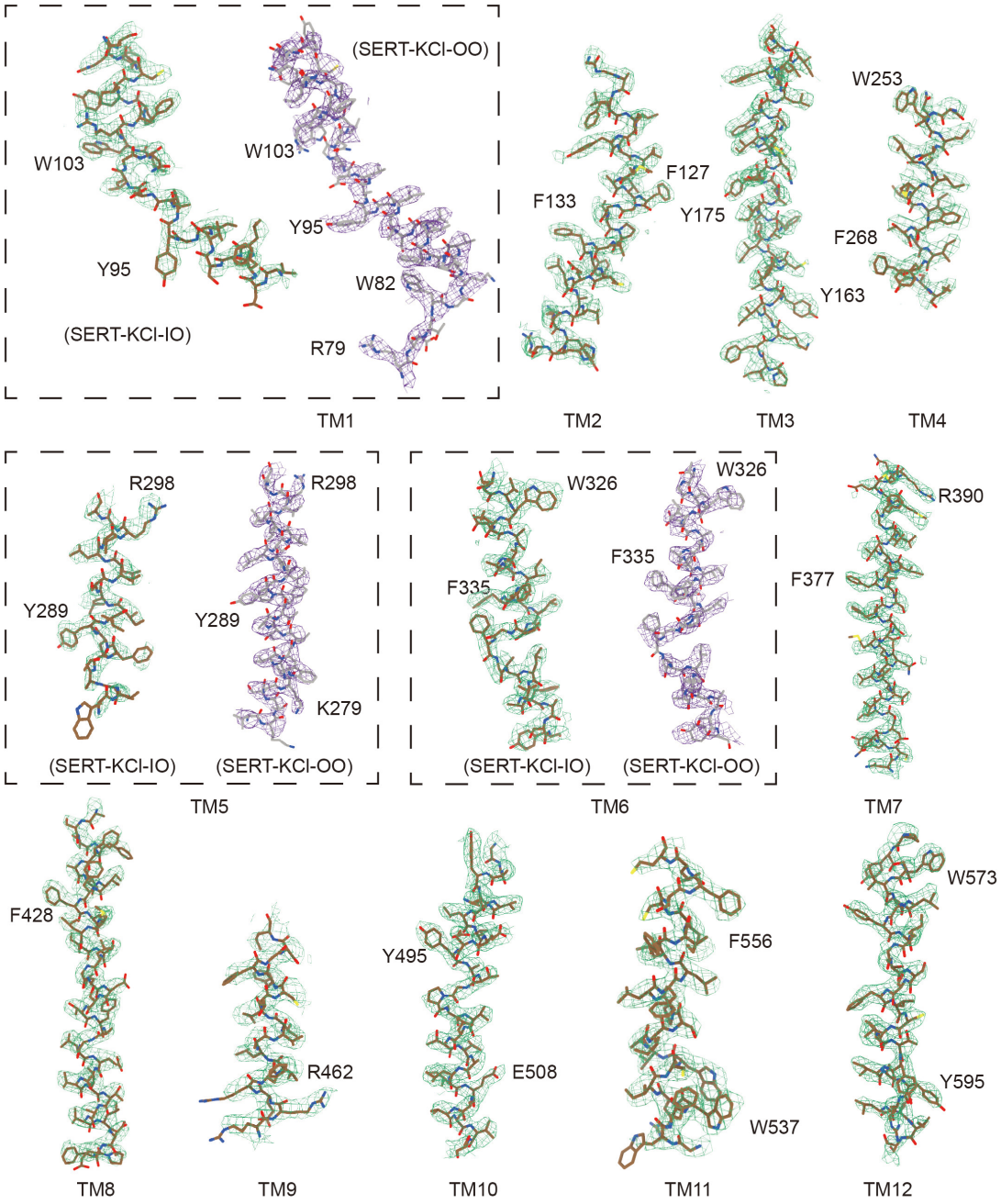

Supplementary Fig. 5 | Representative cryo-EM densities of SERT structures. Representative cryo-EM densities for the TM segments of SERT in KCl, shown separately for the inward and outward states. The densities are contoured at 5.2 σ.

Supplementary Table 1. | Cryo-EM data collection, refinement and validation statistics of SERT.

	SERT-NaCl	SERT-KCl IO	SERT-KCl OO
Data collection and processing			
Magnification		81000	
Voltage (kV)		300	
Electron exposure (e^{-}/Å^2)		~50	
Defocus range (μm)		-1.4~-1.8	
Pixel size (Å)		1.0825	
Symmetry imposed		C1	
Raw movies	3,142	1,817	
Particle Number	251,580	671,549	163,536
Map resolution (Å)	3.10	2.88	3.22
Refinement and Validation			
Protein residues	539	533	539
Ligand	5-HT:2	5-HT:2	5-HT:2
	Cl^-:1	Cl^-:1	
	Na^+:2	K^+:1	
	NAG:1	NAG:1	NAG:1
B factors (Å^2)			
Protein	35.71	70.36	63.43
Ligand	42.55	76.25	69.85
R.m.s. deviations			
Bond lengths (Å)	0.005	0.007	0.005
Bond angles (°)	0.626	0.691	0.676
MolProbity score	1.85	1.92	2.01
Clashscore	8.4	9.8	11.05
Ramachandran plot			
Favored (%)	94.23	93.92	92.92
Allowed (%)	5.77	6.08	7.08
Disallowed (%)	0	0	0
PDB code	8WHF	8WHE	8WHD
EMDB code	EMD-37542	EMD-37541	EMD-37540